Thermodynamic Modeling of Condensed Salts and Silicates at High Temperatures

Bing Liu, Larry L. Baxter, John L. Oscarson, and Reed M. Izatt

Departments of Chemical Engineering and
Chemistry & Biochemistry

Brigham Young University

Ash Deposition

- **Thermal converter slagging/fouling strongly influences design and operation.**

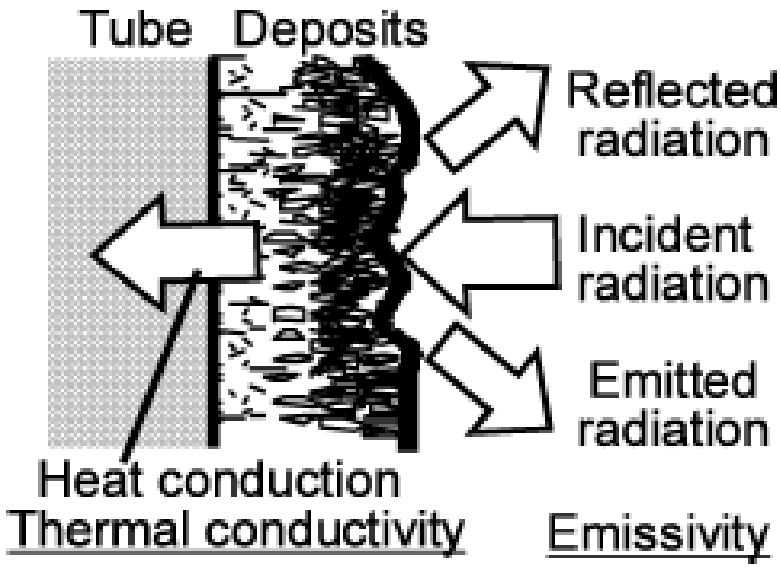

Major Inorganic Compounds in Coals

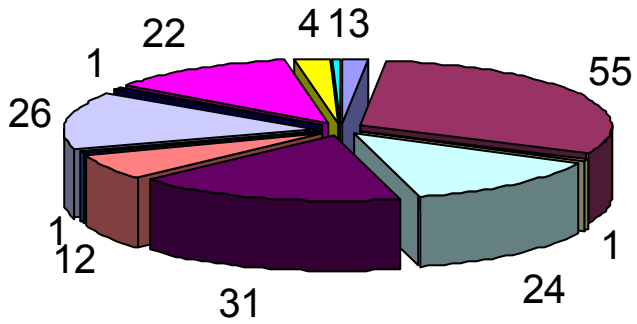

Low Rank

- Sulfides
- Halides
- Hydroxides
- Sulfates
- Phosphates
- Low Melting
- Oxides and Hydroxides
- Oxides
- Carbonates
- Silicates
- High Melting
- Mineraloids

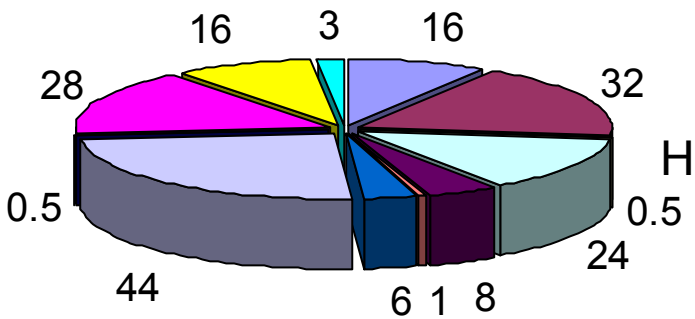

High Rank

Fusion temperature of ash varies with coal

Measuring phase equilibria of ash/slags is difficult and costly over a wide range of compositions and temperatures

Thermodynamic Models

Few ash deposits are in equilibrium, but equilibrium represents an important limiting behavior

Thermodynamic models help describe

- Fusion temperatures
- Deposition rates and mechanisms
- Operating regime

Objectives

- Develop a thermodynamic model to correlate/predict high-temperature phase diagrams

- Validate the model using available experimental data

Pure Component Properties Are Needed

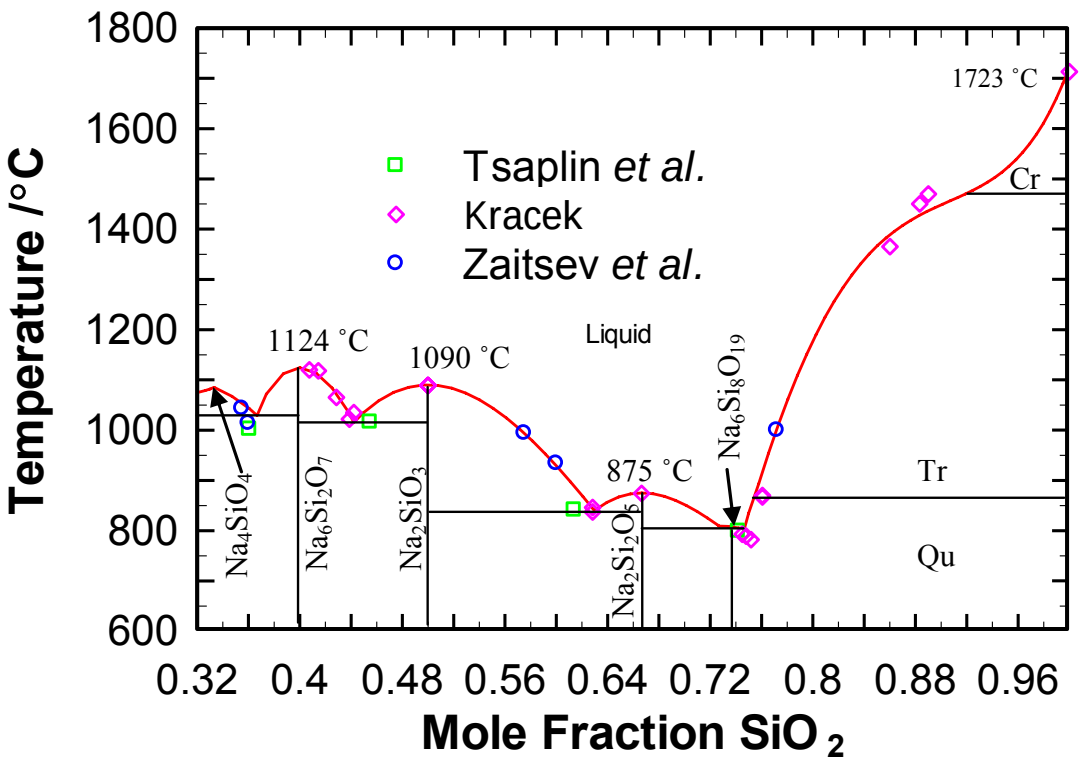

Na_2O-SiO_2 phase diagram.

- The melting point of the mixture may lie several hundred degrees below pure component data
- Intermediate compound properties may not have been measured or be available in a standard thermodynamic database

Extrapolation is Unreliable

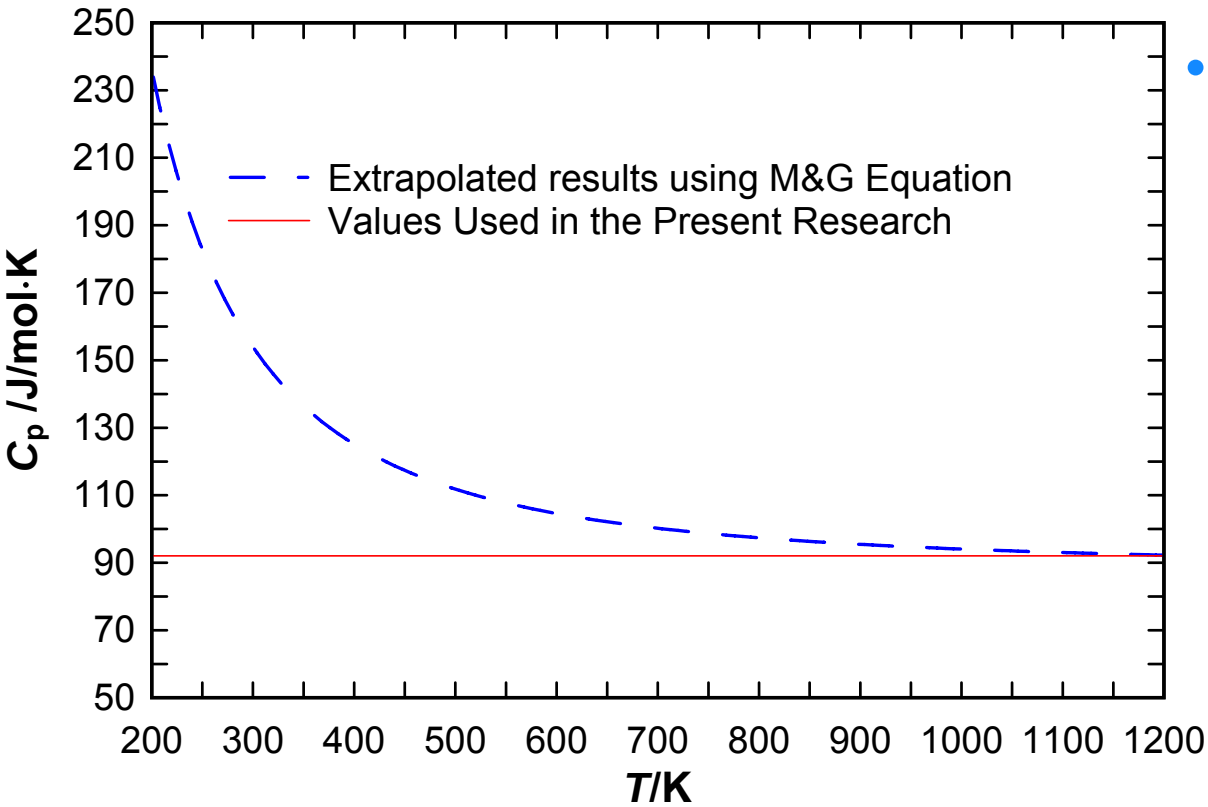

- **The overestimated heat capacity results may lead to errors in the phase diagram expectations.**

Comparison of Liquid $MgCl_2$ Heat Capacities

Pure Component Properties (Cont.)

- **The FACTsage heat capacity equation form is used to calculate the heat capacities of pure components**

$$C_p = a + b\times10^{-3}T + \frac{c\times10^{5}}{T^2} + \frac{d}{\sqrt{T}} + e\times10^{-6}T^2 + f\times10^{-9}T^3$$

- **Heat capacities at unstable conditions (supercooled/superheated) can be approximated using thermodynamic identities in the cases where no literature data exist**

$$\Delta_{tr}G = \Delta_{tr}H - T\Delta_{tr}S$$

$$\Delta C_P = C_{P,L} - C_{P,S} = -T\left(\frac{d^2\Delta_{tr}G}{dT^2}\right) \approx 0$$

- **Properties of the intermediate compounds can be optimized based on other kinds of measured thermodynamic properties (*e.g.*, phase diagram data)**

Liquids: Modified Quasi-chemical Model

- In a binary system composed of components *A* and *B*, the mixing Gibbs energy change can be accounted for by a quasi-chemical reaction:

  (A-A) + (B-B) = 2 (A-B) $\quad \Delta g_{AB}$

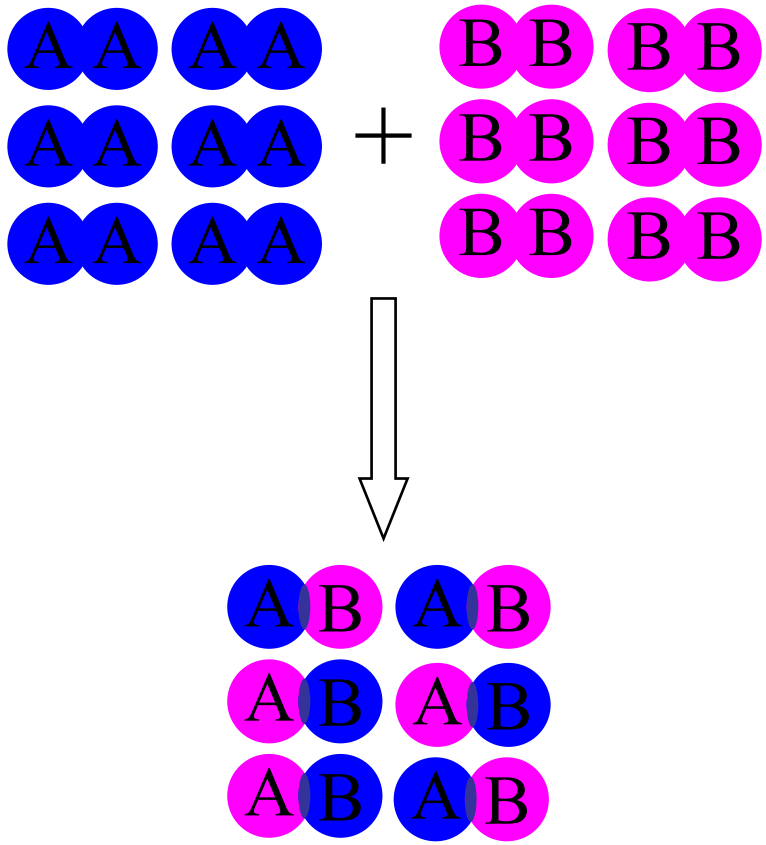

- The Total Gibbs energy of the system is:

$$G = (x_A g_A^o + x_B g_B^o) - T\Delta S^{config} + (n_{AB}/2)\Delta g_{AB}$$

G: total Gibbs energy of the solution
T: temperature
x_i: mole fraction of the components
g_i^o: Gibbs energy of the pure component
ΔS^{config}: configurational entropy
n_{AB}: number of AB pairs in the solution
Δg_{AB}: nonconfigurational gibbs energy change

Modified Quasi-chemical Model (Cont.)

- The configurational entropy accounts for the random mixing contribution of the compounds/pairs in the system, and is usually expressed as a function of mole fractions of the initial compounds and a a function of pairs.

$$\Delta S^{\text{config}} = -R(x_{\text{A}} \ln x_{\text{A}} + x_{\text{B}} \ln x_{\text{B}}) - R\left(n_{\text{AA}} \ln \frac{x_{\text{AA}}}{Y_{\text{A}}^2} + n_{\text{BB}} \ln \frac{x_{\text{BB}}}{Y_{\text{B}}^2} + n_{\text{AB}} \ln \frac{x_{\text{AB}}}{2Y_{\text{A}}Y_{\text{B}}} \right)$$

$$Y_{\text{A}} = x_{\text{AA}} + \frac{x_{\text{AB}}}{2} \qquad Y_{\text{B}} = x_{\text{BB}} + \frac{x_{\text{AB}}}{2}$$

x_{i} : mole fraction of component i in the solution

n_{ij} : number of ij pairs in the solution

Y_{i} : equivalent fraction of pairs with component i

x_{ij} : mole fraction of ij pairs

Modified Quasi-chemical Model (Cont.)

- **Δg_{AB} is the nonconfigurational Gibbs energy change due to the reaction.**

$$\Delta g_{AB} = \sum_{i=0}^{n} g_i x_A{}^i \quad \text{or}$$

$$\Delta g_{AB} = g_0 + \sum_{i=1}^{n} g_i Y_A{}^i + \sum_{j=1}^{n} g_j Y_B{}^j \quad \text{or}$$

$$\Delta g_{AB} = g_0 + \sum_{i=1}^{n} g_i x_{AA}{}^i + \sum_{j=1}^{n} g_j x_{BB}{}^j$$

  - **The coefficients (g_0, g_i, g_j) of Δg_{AB} are optimized using available thermodynamic data (enthalpies, entropies, phase equilibrium data etc.)**

Binary Salt System Example I

Liquid solution is in equilibrium with pure solids

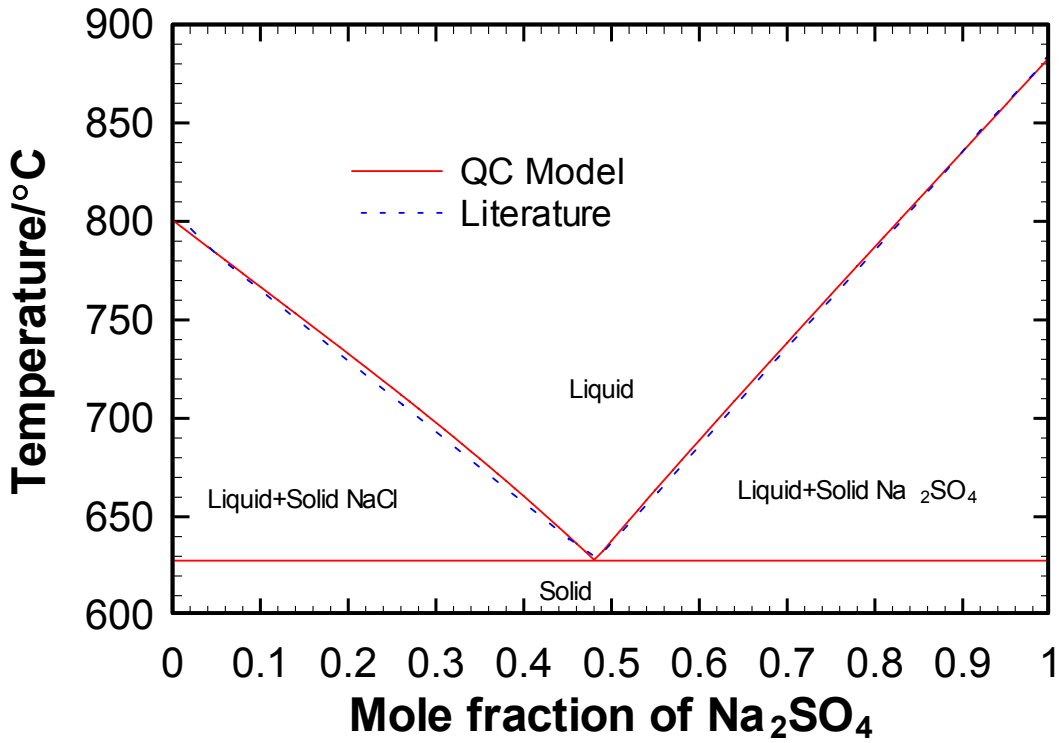

T-x phase diagram of the Na_2SO_4-NaCl system. The dashed line is calculated using the smoothed data of Dessureault *et al.*'s

Binary Salt System Example II

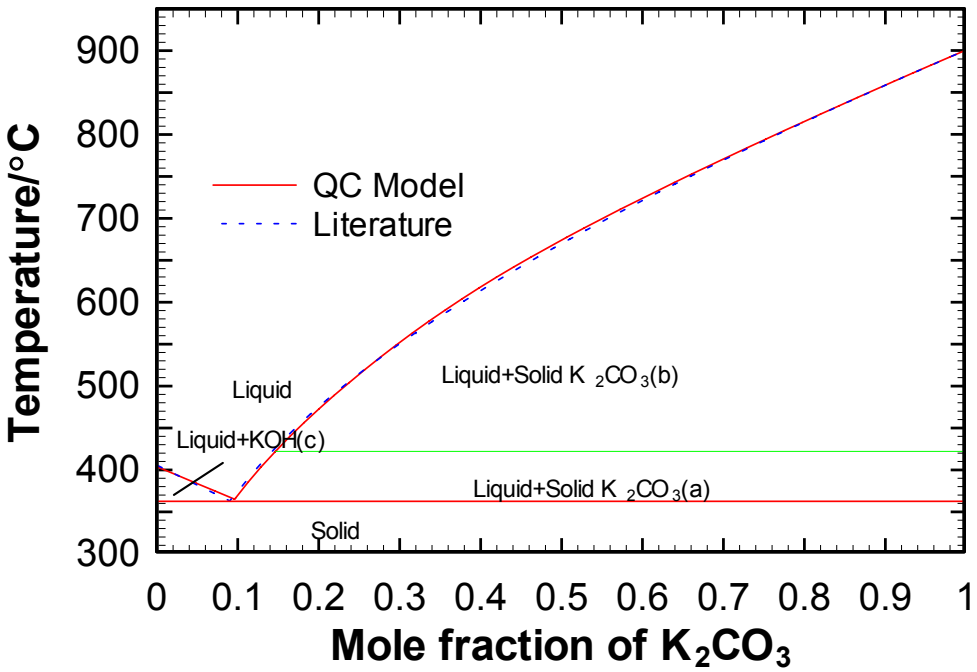

T-x phase diagram of the K_2CO_3-KOH system. The dashed line is calculated using the smoothed data of Dessureault *et al*.

- Liquid solution is in equilibrium with pure solids (different crystals)
- The minimum melting point of the system is near the KOH side resulting from the relatively large absolute Gibbs energy value of K_2CO_3

Eutectic Point Comparisons

- A **eutectic** or **eutectic mixture** is a mixture of two or more phases at a composition that has the lowest **melting point**.
- Agreement of the **eutectic points** (calculated using the model and literature data) shows the ability of the model to correlate phase diagrams

System ($A-B$)	Model x_B	Literature x_B	Model T_{eu} , ˚C	Literature T_{eu}, ˚C
$NaCl\text{-}Na_2CO_3$	0.449	0.41−0.47	632.96	632−645
$KCl\text{-}K_2CO_3$	0.358	0.35−0.38	629.69	623−636
$KCl\text{-}K_2SO_4$	0.260	0.23−0.29	690.89	688−694
$NaCl\text{-}Na_2SO_4$	0.481	0.45−0.48	627.80	623−634
$KOH\text{-}K_2CO_3$	0.091	0.09−0.10	362.48	360-367

Binary Salt System Examples II

Liquid solution is in equilibrium with solid solution

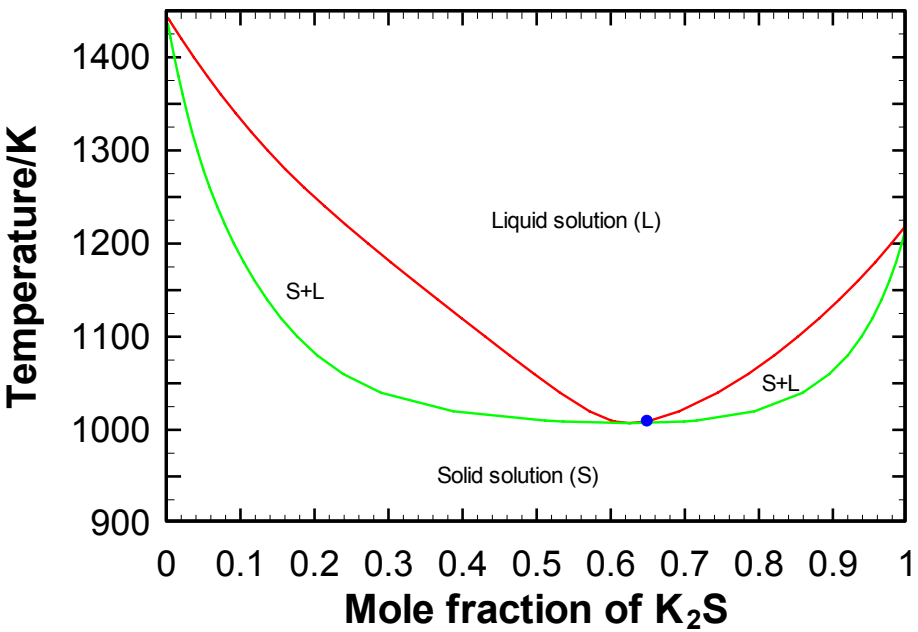

Liquid-solid solution phase diagram of the K_2S-Na_2S system. ● from Mäkipää and Backman

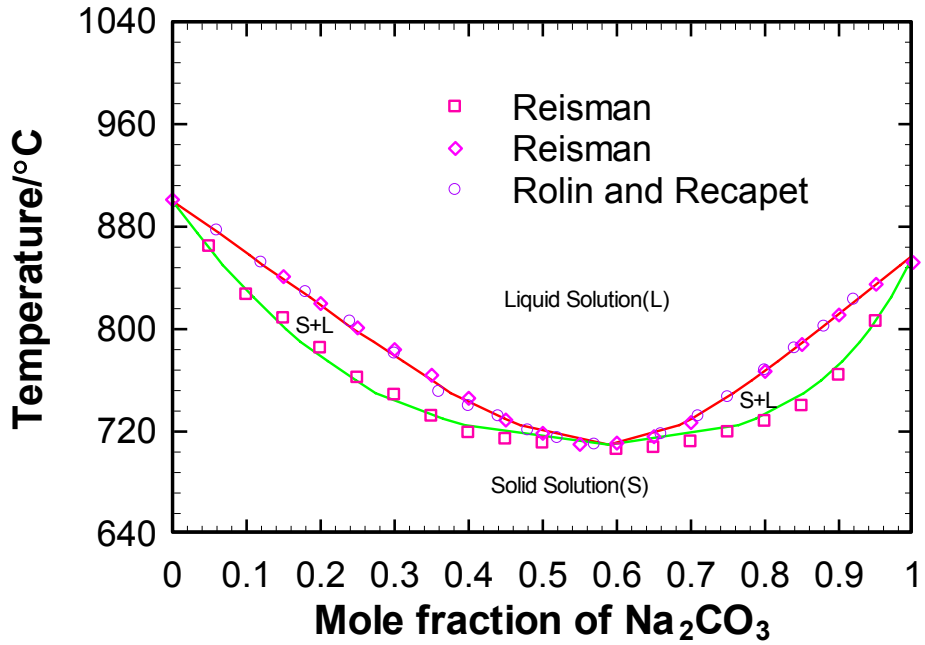

Liquid-solid solution phase diagram of the K_2CO_3-Na_2CO_3 system.

K_2O-SiO_2 Phase Diagram

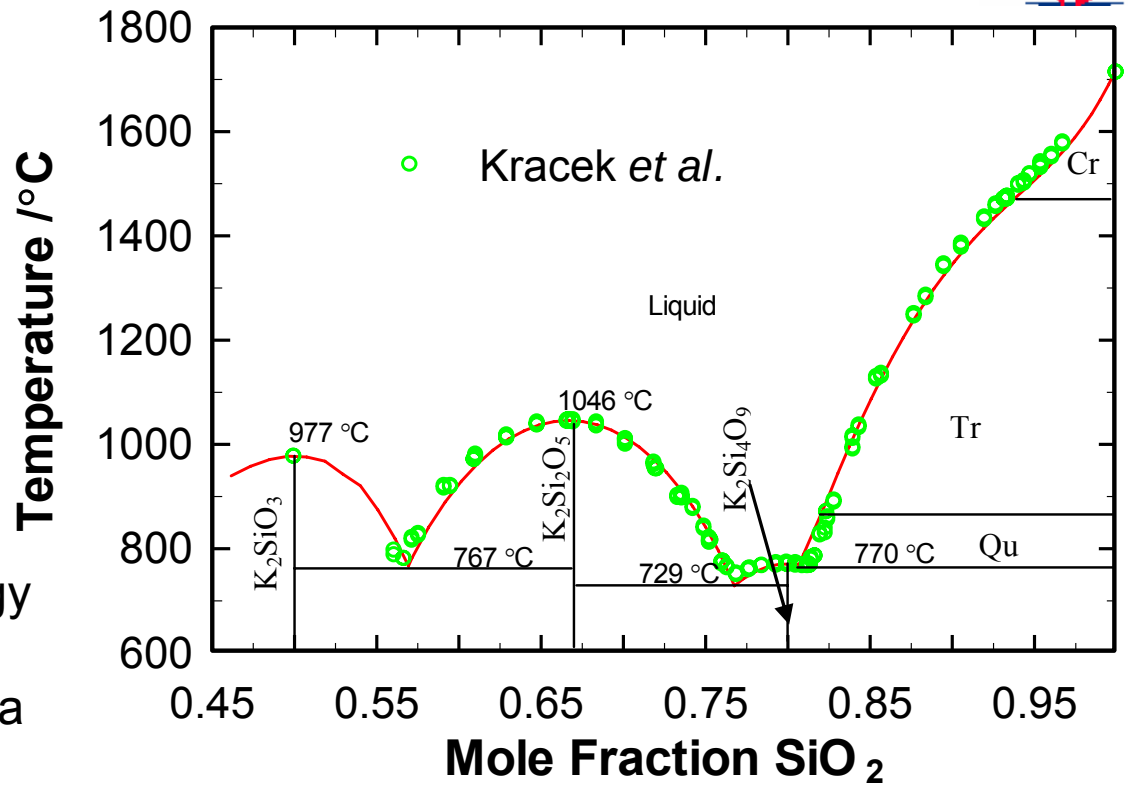

- Properties of many intermediate silicates cannot be measured and must be optimized based on data in the regions where there is no formation of these compounds.

- The equation of Gibbs energy of the $K_2Si_2O_5$ is optimized using the equilibrium *T*~*x* data based on the following reaction:

$$K_2O(l) + 2SiO_2(l) = K_2Si_2O_5(s) \quad \Rightarrow \quad G_{K_2Si_2O_5(s)}(T) = u_{K_2O(l)}(x,T) + 2u_{SiO_2(l)}(x,T)$$

$CaO\text{-}SiO_2$ Phase Diagram

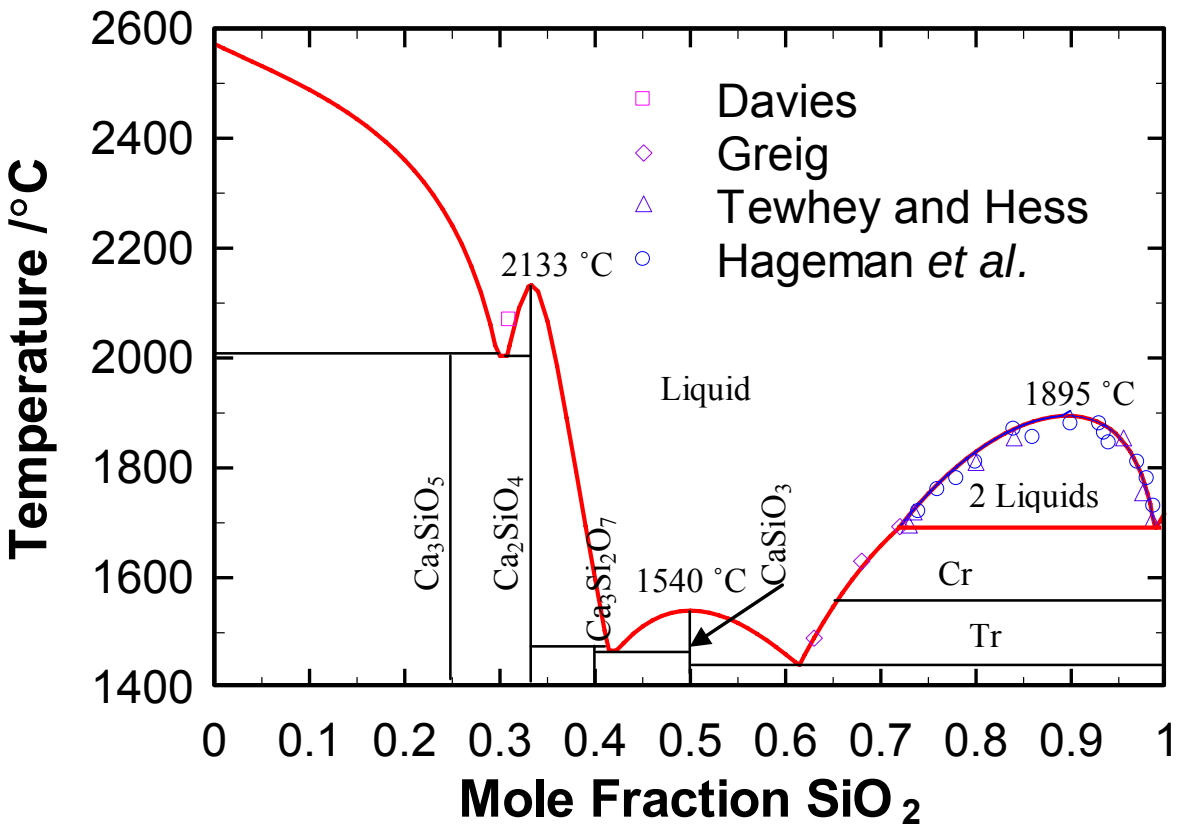

- The high melting temperature of pure CaO accounts for the high melting point in CaO-rich systems
- The thermodynamic properties (e.g., Gibbs energy and melting point values) of the intermediate compounds are obtained by optimizing the phase equilibrium data

$AlO_{1.5}$-SiO_2 Phase Diagram

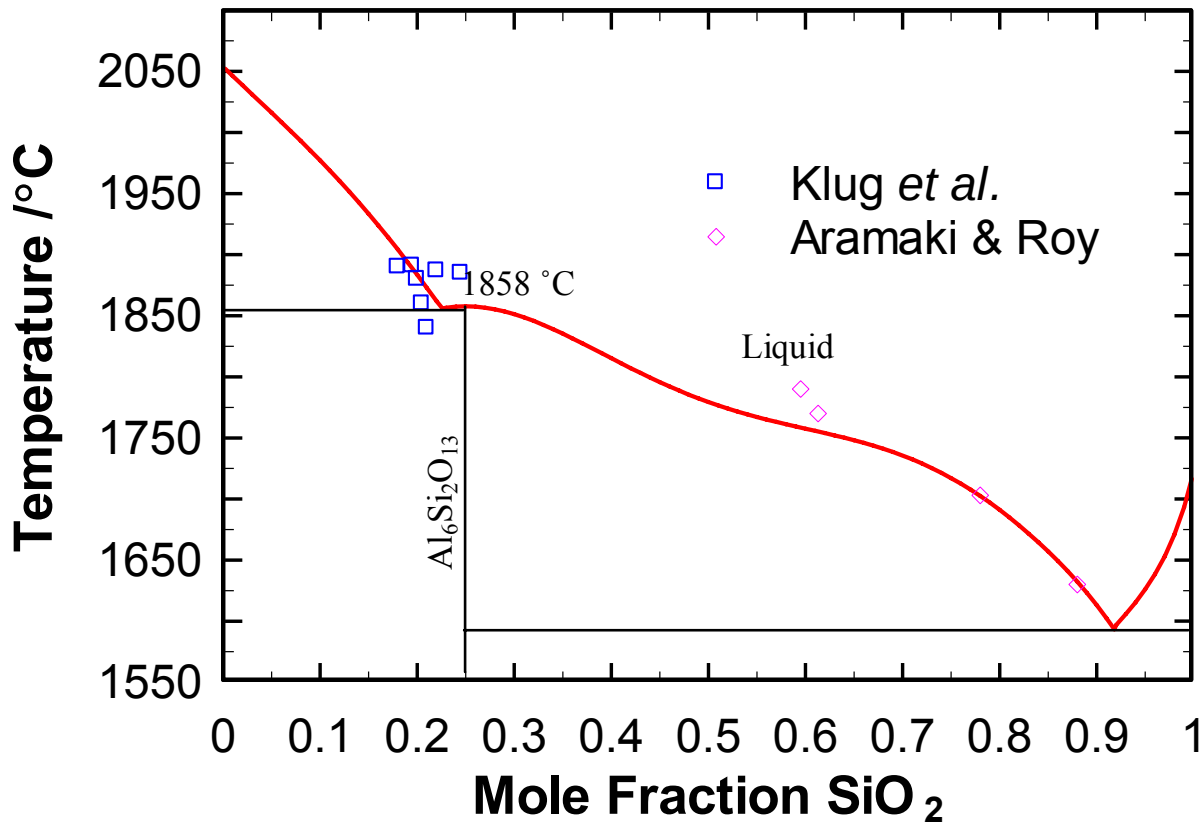

- More experiments are needed to better correlate the phase diagrams in the intermediate compounds regions
- The intermediate compound $Al_6Si_2O_{13}$ may account for the slow decrease of the melting point with increasing SiO_2 concentrations

$FeO\text{-}SiO_2$ Phase Diagram

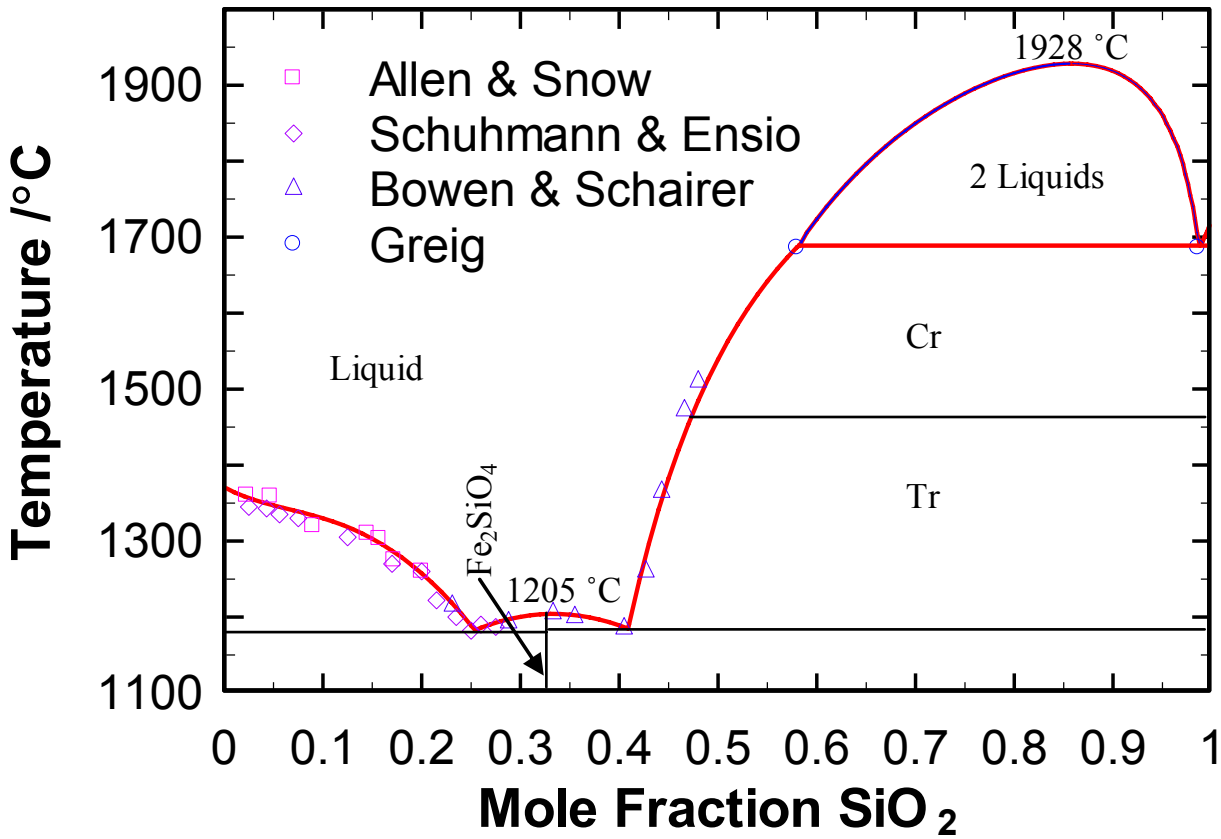

The relatively low melting point of Fe_2SiO_4 implies that the association between FeO and SiO_2 is not as strong as those between many other metallic oxides (CaO, Al_2O_3 etc.) and SiO_2

Comparison of melting points of several associated compounds in silicate systems

Component	Calculated MP (˚C)	Literature MP (˚C)
K_2SiO_3	977	976–977
$K_2Si_2O_5$	1046	1045–1046
$K_2Si_4O_9$	770	769–771
Na_2SiO_3	1090	1090–1100
$Na_2Si_2O_5$	875	875
Na_4SiO_4	1085	1085
$Na_6Si_2O_7$	1124	1124
Ca_3SiO_4	-	1800–2149
Ca_2SiO_4	2133	2130–2145
$CaSiO_3$	1540	1540–1544

Eutectic Points in Silicate Systems

Type	Calculated EP		Literature EP	
	T (°C)	$x(SiO_2)$	T (°C)	$x(SiO_2)$
K_2SiO_3-$K_2Si_2O_5$	767	0.569	780–781	0.567
$K_2Si_2O_5$-$K_2Si_4O_9$	729	0.767	743	0.764–0.766
$K_2Si_4O_9$-SiO_2(Qu)	770	0.807	770	0.805
Na_4SiO_4-$Na_6Si_2O_7$	1029	0.367	1002	0.361
$Na_6Si_2O_7$-Na_2SiO_3	1015	0.442	1016	0.455
Na_2SiO_3-Na_4SiO_4	839	0.623	841–847	0.614–0.63
$Na_6Si_8O_{19}$-SiO_2(Qu)	804	0.747	794–799	0.742
Ca_3SiO_5-Ca_2SiO_4	2023	0.295	2057–2060	0.273–0.30
$Ca_3Si_2O_7$-$CaSiO_3$	1467	0.422	1450–1460	0.42–0.445
$CaSiO_3$-SiO_2(Tr)	1441	0.615	1441–1444	0.61–0.635

Summary of Current Progress

- A modified quasi-chemical model taken from the literature has been used to correlate phase diagrams of molten salts and silicates
- The validity of the model has been tested and verified using many binary systems
- Optimal modeling parameters of many binary systems potentially related to the coal ash components have been found for use in later multicomponent modeling
- Thermodynamic properties of many pure compounds have been collected, approximated, or optimized.

References

- Allen, W.C.; R.B. Snow, *J. Am. Ceram. Soc.*, 1955, 38, p.264.
- Aramaki, S.; R. Roy, *J. Am. Ceram. Soc*., 1962, 45, p.229.
- Bowen, N.L.; J.F. Schairer, *Am. J. Sci.*, 1932, 24, p177.
- Davies, M. W. Ph.D. Thesis, Imperial College, London, 1955.
- Dessureault, Y.; Sangster, J.; Pelton, A. D., *J. Phy. Chem. Ref. Data* 1990, 19, (5), p.1149.
- Donald L. Bonk, NETL, U. S. Department of Energy.
- Greig, J. W., *Am. J. Sci.* 1927, 13, p1, p.133.
- Greig, J. W., *Am. J. Sci.* 1927, 14, (5), p.473.
- Hageman, V.B.M.; G.J.K. vanden Berg; H.J. Janssen; H.A.J. Oonk, *Phys. Chem. Glasses*, 1986, 27, p.100.
- Klug, F.J.; S. Prochazka; R.H. Doremus, *J. Am. Ceram. Soc*., 1987, 70, p.750.
- Kracek, F. C., *J. Phy. Chem.* 1930, 34, p.1583.
- Kracek, F. C.; Bowen, N. L.; Morey, G. W., *J. Phys. Chem.* 1937, 41, p.1183.
- Reisman, A., *J. Am. Chem. Soc.* 1959, 81, p.807.
- Rolin, M.; Recapet, J. M., *Bulletin de la Societe Chimique de France* 1964, (9), p. 2104.
- Schuhmann, R.; P. Ensio, *J. Met.*, 1951, 3, p401.
- Tewhey, J.D.; P.C. Hess, *Phys. Chem. Glasses*, 1979, 20, p.41
- Mäkipää, M.; Backman, R., In *9th International Symposium on Cossosion in the Pulp and Paper Industry*, 1998.
- Tsaplin, A. A.; Zaitsev, A. I.; Shelkova, N. E.; Mogutnov, B. M., *Juelich, Reihe Energietechnik/Energy Tech.* 2000, 15, p.59.
- Zaitsev, A. I.; Shelkova, N. E.; Lyakishev, N. P.; Mogutnov, B. M., *Phy. Chem. Chem. Phy.* 1999, 1(8), p.1899.

Thank You